Petroleum Science 20 (2023) 3100–3109

Contents lists available at ScienceDirect

Petroleum Science

journal homepage: www.keaipublishing.com/en/journals/petroleum-science

Original Paper

Experimental studies on rock failure mechanisms under impact load by single polycrystalline diamond compact cutter

Zhao-Sheng Ji [a], Jin-Bao Jiang [a], Huai-Zhong Shi [b, *], Bang-Min Li [a]

[a] Drilling Engineering Technology Research Institute, Sinopec Zhongyuan Petroleum Engineering Company, Puyang, Henan, 457001, China
[b] State Key Laboratory of Petroleum Resources and Prospecting, Beijing, 102249, China

ARTICLE INFO

Article history:
Received 31 August 2022
Received in revised form
15 January 2023
Accepted 6 April 2023
Available online 10 April 2023

Edited by Jia-Jia Fei

Keywords:
Percussive drilling
PDC cutter
Drop test
Failure mechanism
Subsurface cracks

ABSTRACT

Percussive drilling shows excellent potential for promoting the rate of penetration (ROP) in drilling hard formations. Polycrystalline diamond compact (PDC) bits account for most of the footage drilled in the oil and gas fields. To reveal the rock failure mechanisms under the impact load by PDC bits, a series of drop tests with a single PDC cutter were conducted to four kinds of rocks at different back rake angles, drop heights, drop mass, and drop times. Then the morphology characteristics of the craters were obtained and quantified by using a three-dimensional profilometer. The fracture micrographs can be observed by using scanning electron microscope (SEM). The distribution and propagation process of subsurface cracks were captured in rock-like silica glass by a high-speed photography system. The results can indicate that percussive drilling has a higher efficiency and ROP when the rock fractures in brittle mode. The failure mode of rock is related with the type of rock, the impact speed, and the back rake angle of the cutter. Both the penetration depth and fragmentation volume get the maximum values at a back rake angle of about 45°. Increasing the weight and speed of falling hammer is beneficial to improving the rock breaking effects and efficiency. The subsurface cracks under the impact load by a single PDC cutter is shaped like a clamshell, and its size is much larger than the crater volume. These findings can help to shed light on the rock failure mechanisms under the impact of load by a single PDC cutter and provide a theoretical explanation for better field application of percussive drilling.

1. Introduction

Due to the instantaneous stress concentration effect, rocks are more prone to breaking under impact loads (Altindag, 2010; Derdour et al., 2018; Song et al., 2021; Yang et al., 2018; Zhang and Zhao, 2014). Based on this principle, percussive drilling technology has been widely used for rock fragmentation and subground drilling in the civil and mining industry (Buyuksagis and Goktan, 2007; Gee et al., 2012; Ji et al., 2021). It also presents significant potential for promoting the rate of penetration (ROP) when drilling hard formations in oil and gas industries (Chen and Yue, 2015; Fan et al., 2011; Li et al., 2017; Jiang et al., 2020; Pavlovskaia et al., 2015), as well as the geothermal industry (Beswick et al., 1987; Wu et al., 2019). The principle behind percussive drilling is straightforward: the repeated collision between two elastic bodies generates pulse impacts that can be transmitted to the drill bits. As a result of dynamic indentation, the drill bit penetrates the rock by crushing and chipping. A thorough comprehension of the dynamic bit-rock interaction mechanism is of great significance to the design of the impact tools to improve drilling efficiency.

Over the last two decades, numerous experimental studies have been conducted to reveal the rock failure mechanisms in percussive drilling. These experiments were essential for observing rock fragmentation phenomena and developing models to study the mechanisms of rock failure caused by tools (Liao et al., 2021; Wang et al., 2006). With the development of computational capacity, numerical analysis has become an essential method to study the mechanism of rock failure (Dong and Chen, 2018; Jiang et al., 2014, 2019; Karfakis and Ouyang, 1994). Liu et al. (2008) investigated the rock failure process induced by different bits with one to multiple buttons using the rock and tool interaction code (R-T2D). Saksala et al. (2014) built a finite element model to simulate the percussive drilling of a triple-button bits into Kuru granite, presenting the distribution of tensile damage, compressive damage, and

* Corresponding author.
E-mail address: shz@cup.edu.cn (H.-Z. Shi).

https://doi.org/10.1016/j.petsci.2023.04.008

Nomenclature

β	Back rake angle of PDC cutter
E_{spe}	Specific energy
D_{inden}	Indentation energy
V_{frag}	Fragmentation volume
m_{dp}	Mass of the drop hammer
g	Gravitational acceleration
B	Brittleness index
σ_c	Uniaxial compressive strength
σ_t	Tensile strength
h_{dp}	Drop height of drop hammer

volumetric plastic strain at different impact loads and bit geometry parameters. Additionally, a significant amount of effort has been devoted to the macro relationship between the contact force and displacement in percussive drilling.

Researchers have focused on studying the contact force between the bit and rock in percussive drilling through a combination of experimental studies (Ajibose et al., 2015; Bilgin et al., 2006), numerical analyses (Depouhon et al., 2015; Dong and Chen, 2018), and theoretical models (Franca, 2011; Hustrulid and Fairhurst, 1971; Li et al., 2017). Ji et al. (2020) developed an improved drifting oscillator model to describe the contact force at the indentation surface and predict the penetration process of the bit. Ajibose et al. (2015) investigated the force versus penetration displacement for a bit with conical and spherical inserts. These experimental results have been verified by comparing them with theoretical results. Song et al. (2019) established a three-dimensional percussive model using the finite element method to present the contact force versus penetration displacement at different load velocities and durations. In this model, the bit with spherical teeth were selected to indent into the rock.

It is noticeable that most of research on percussion drilling focuses on spherical or conical teeth. However, polycrystalline diamond compact (PDC) bit is the primary rock breaking tool in exploring and exploiting deep oil, gas, and geothermal resources (Abbas, 2018; Hareland et al., 2009; Huang et al., 2019; Kuang et al., 2016). Therefore, it is essential to study the indentation process of PDC teeth.

To reveal the rock failure mechanisms under the impact load of a single PDC cutter, a series of drop tests have been conducted. The morphology characteristics of the crater were obtained and quantified by a three-dimensional profilometer. The fracture micrographs have been observed by using scanning electron microscope (SEM). The distribution and propagation processes of cracks were captured in rock-like silica glass by using a high-speed photography system. Take the penetration depth, fragmentation volume, and specific energy as evaluation indexes, the influences of back rake angle of the cutter, rock type, impact velocity, impact mass and impact times, on ROP and drilling efficiency of percussive drilling were studied.

2. Experimental setup and scheme

2.1. Experimental setup

Fig. 1 shows the setup schematic of drop tests. This setup mainly comprises five parts: the drop part, the lifting part, the data acquisition part, the control part, and the post-processing part. The lifting part consists of the motor, the lifting rod, and the electromagnet. In the lifting process, the electromagnet is electrified, which can draw the lifting part and the drop part tightly together by strong magnetism. The drop hammer rises to the specified height by the lifting rod and the motor, which follows the command from the control terminal. Then the electromagnet is de-energized, and its magnetism disappears. Due to gravity, the drop part begins to fall. The drop part includes clump weight, the single PDC cutter, and its clapping device. This part obtains a specific speed by drop action. Then the drop action is transformed into the impact load to impress the single PDC cutter into the rock. Thus, the impact action in percussive drilling is simulated. The related data in the rock fragmentation process by the impact load are monitored and recorded by the data acquisition system. For quantifying the topography characteristics of craters and observing the fracture microstructure, the broken stones are sent to the post-processing part, which consists of a three-dimensional topography instrument and a SEM.

2.2. Clamping device

A single PDC cutter is used to study on the rock fragmentation mechanism by the impact load as the behavior of the full PDC bit could be an average of the individual cutter's action (Akbari, 2011). Most researchers also use a single cutter in their studies for its concision and simplicity (Cheng et al., 2018). Practical PDC cutters are used to study the impact process more realistically. Special clamping devices are designed to mount the cutter on the testing setup, as shown in Fig. 2 where β is easily known as the back rake angles. We have designed a series of clamping devices to study the influence of back rake angles on the rock fragmentation effect under the impact load. This series involves different back rake angles β of 0°, 10°, 20°, 30°, 40°, 50°, and 60°.

2.3. Test scheme and sample preparation

Drop tests have been carried out on the samples of sandstone, granite, shale, and marble. The mechanic parameters of these rocks are shown in Table 1. The specimens are made into cubes with dimensions 100 mm × 100 mm × 100 mm. In addition to the rock type and the back rake angle mentioned in the previous section, the influences of other parameters, such as the drop height h_{dp}, the impact times n_{dp} and mass m_{dp} of the drop part, on the fragmentation effect also be analyzed. The drop height can be specified in the control terminal as different values of 240, 280, 320, 360, 400, and 440 mm. The drop mass can be evaluated by adjusting the block number of the clump weight. Each block of the clump weight weighs 0.5 kg, and the mass of 11, 10, 9, 8, 7, and 6 kg are used in our studies. The times of impacts are also studied, which is designed to be 1, 2, 3, 4, 5, 6 times. To better show the propagation process and distribution of cracks under the impact load, three samples of rock-like silica glass were also prepared. The glass sample has excellent transparency and is more brittle than rock, which can be very helpful for us to capture the subsurface cracks (Cheng et al., 2019).

3. Experimental results and discussion

Drop tests have been conducted to study the influences of the rock type, back rake angle, the mass and height of the drop part, and the impact times on the fragmentation effect which takes shape, depth, and volume of the craters, and the specific energy into consideration. Drop tests on rock-like silica glass were also performed to study the subsurface cracks.

3.1. Influence of rock type and back rake angle

Drop tests can be carried out on four kinds of rocks, i.e., granite,

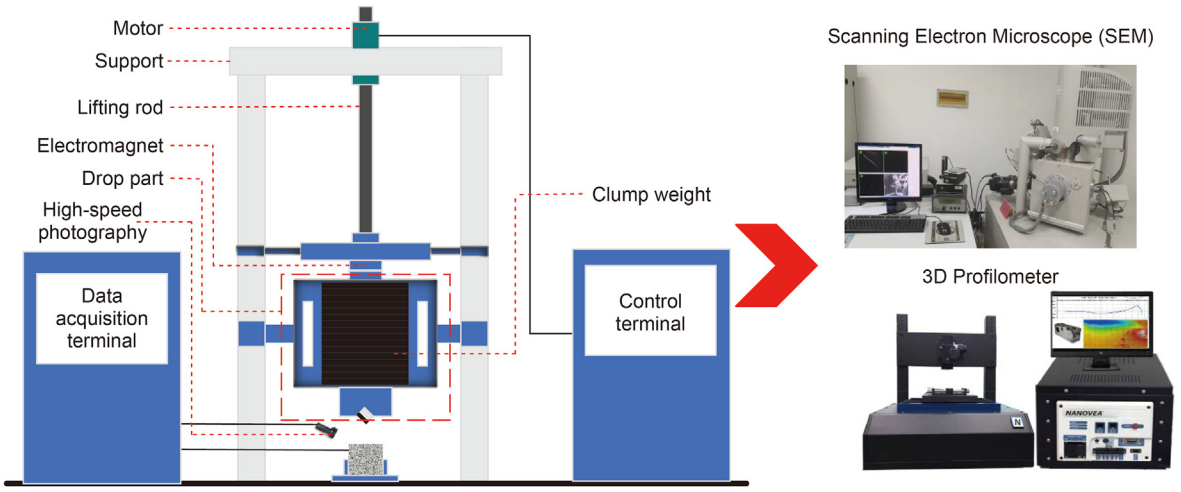

Fig. 1. Schematic of the testing setup.

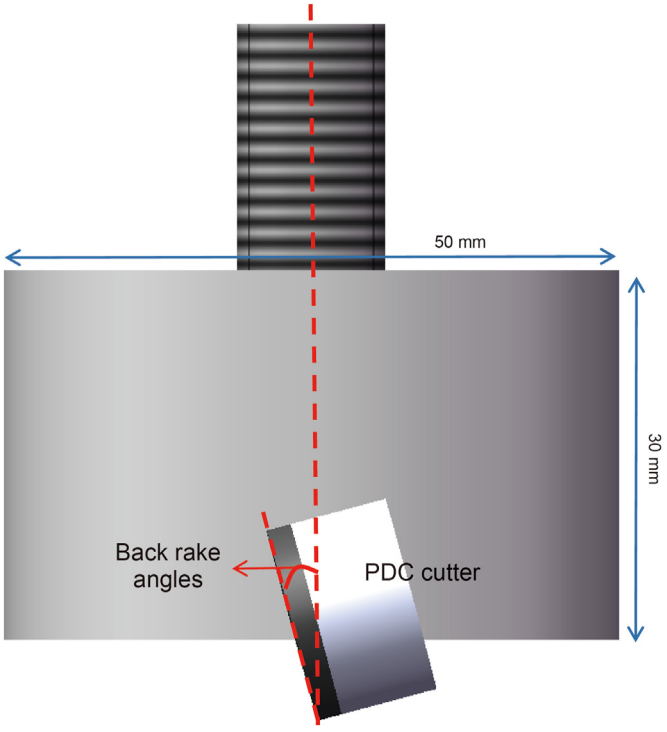

Fig. 2. Schematic diagram of the clamping devices.

marble, shale, and sandstone. Craters are formed on these rock samples after tests. To observe these craters more clearly and directly, we use a three-dimensional profilometer to scan the crater topography. Fig. 3 shows the three-dimensional morphology of the sandstone craters under the impact load of a single PDC cutter with different back rake angles. There are two kinds of failure modes. One is plastic failure caused by compression, and the other is brittle failure caused by tension and shear. These two types of damage coexist in the craters caused by the cutter at a 10° back rake angle. If we define the PDC bit cutting direction in engineering practice as a positive direction, front damage of the cutter is mainly brittle failure, and rear damage of the cutter is mostly plastic failure. The plastic failure surface is relatively flat, and a hard-dense core is formed under the surface. The surface of brittle failure is somewhat rough. With the increase in the back rake angle, the rear part of the crater gradually changes from plastic failure to brittle failure. The failure mode at the front of the cavity also varies, but this change is not so apparent as the rear part.

Fig. 4 shows the variation of quantitative parameters of craters with different back rake angles. The results of all four types of rocks are shown here. The fragmentation volume and penetration depth are obtained from the three-dimensional profilometer. To evaluate the rock breaking efficiency, the specific energy, which refers to the energy required to break a unit volume of rock (Akbari and Miska, 2017), can be calculated by:

$$E_{spe} = \frac{D_{inden}}{V_{frag}} = \frac{m_{dp} g h_{dp}}{V_{frag}} \quad (1)$$

where D_{inden} is the indentation energy, V_{frag} is the fragmentation volume of rock. It should be noted that it is assumed here, namely all the kinetic energy of the drop hammer is used to break the rock.

Curves of penetration depth versus back rake angle are presented in Fig. 4(a). All these curves show a trend of first increasing and then decreasing. All kinds of rocks achieve the maximum value at the back rake angle around 40°–45°, which shows that the cutter has the best penetration effect when it has a back rake angle of 40°–45°. This trend is caused by the change of the contact area

Table 1
Mechanic parameters of rocks.

Rock type	Young's modulus, GPa	Poisson's ratio	Tensile strength, MPa	UCS, MPa	Cohesion strength, MPa	Fraction angle, °
Granite	35.46	0.28	15.2	164.2	37.88	53.18
Sandstone	16.25	0.33	8.5	93.2	21.25	46.02
Shale	57.89	0.18	16.8	174.6	84.11	45.49
Marble	48.21	0.17	8.7	117.5	29.56	54.21
Silica glass	14.85	0.165	\	188.3	\	\

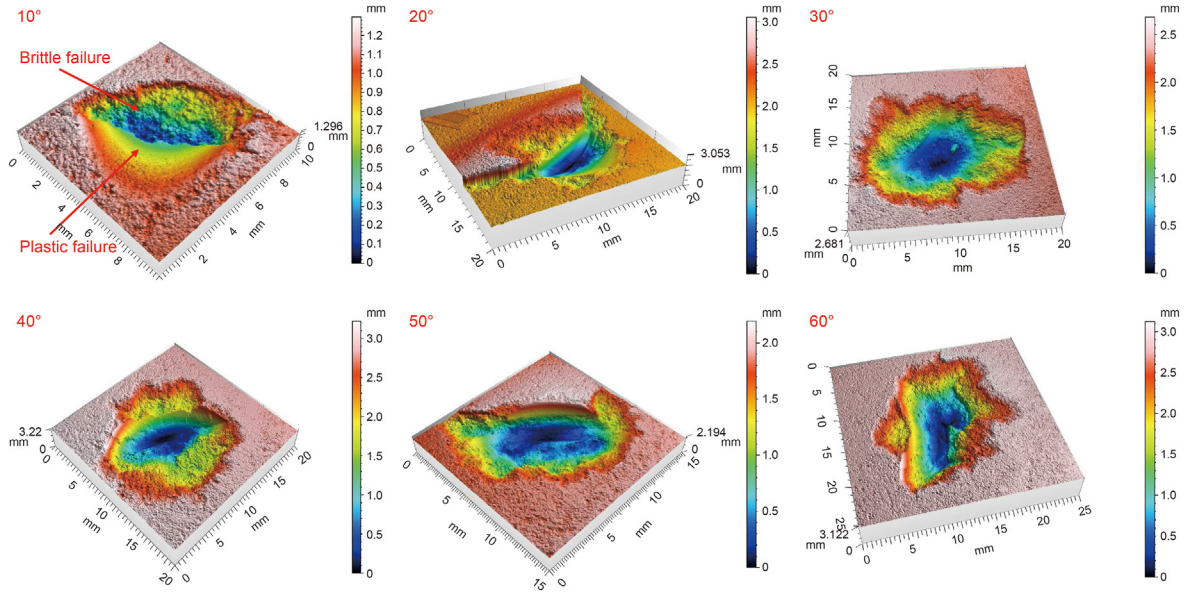

Fig. 3. Surface topography of sandstone crater under a single PDC cutter with different back rake angles.

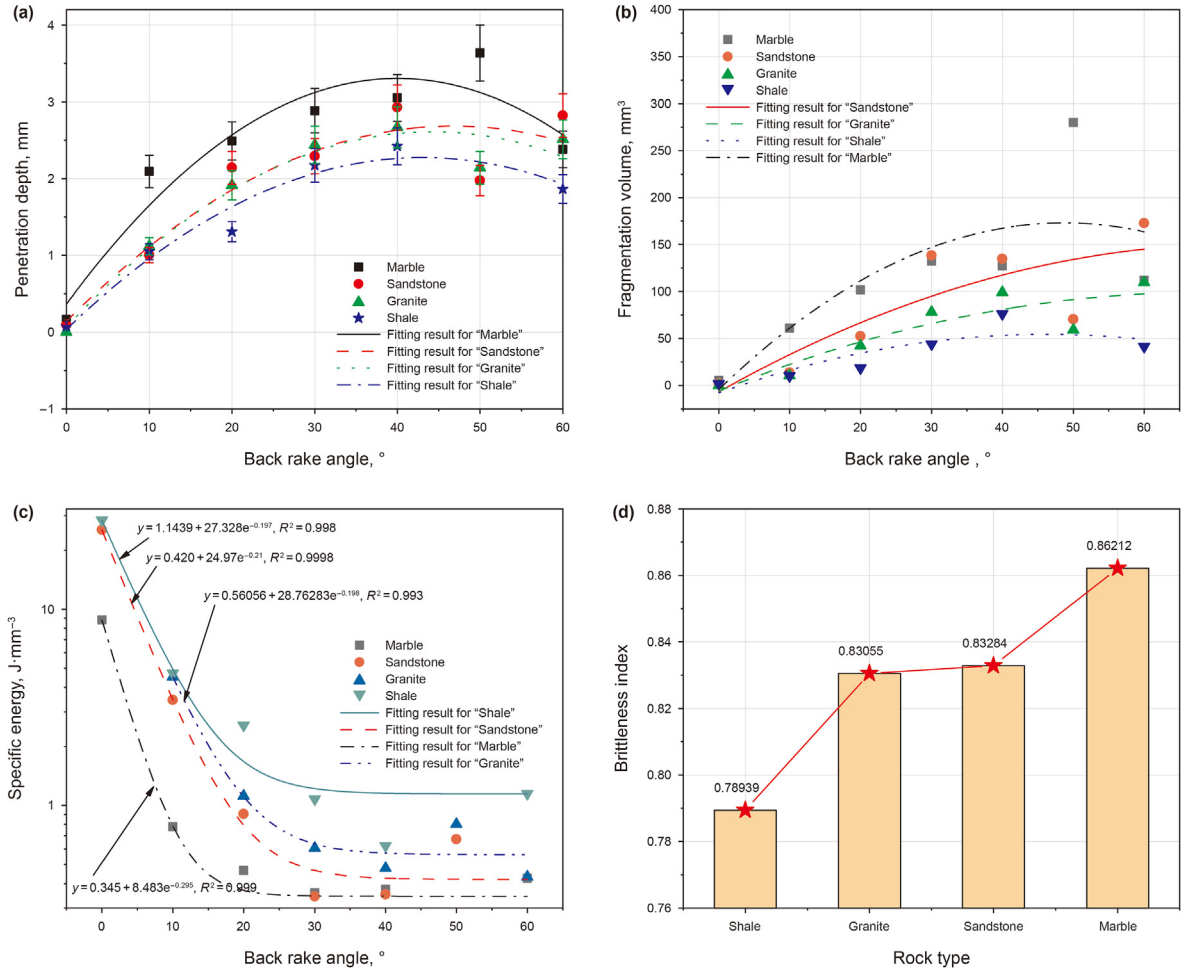

Fig. 4. The relationships between (**a**) penetration depth, (**b**)fragmentation volume, (**c**) specific energy and back rake angle; and (**d**) the brittleness index of different kinds of rocks.

between the cutting teeth and the rock. As the back rake angle increases, the contact area between the side of the cutter and the rock decreases, and the area between the bottom of the cutter and the rock increases. The overall result is that the total contact area

between cutter and rock decreases first and then increases. This law explains why increasing the back rake angle helps drill in hard formation. Cutters with a back rake angle smaller than 20° are often used to cut the regular formation in rotary-percussive drilling (RPD). When the rock becomes hard, the back rake angle needs to be increased to maintain the regular cutting depth. Curves of fragmentation volume versus back rake angle in Fig. 4(b) displays an overall increases trend. In the analysis range, the fragmentation volume of marble and shale shows a slight downward trend after the end of the upward trend with the increase of the back rake angle. The maximum values are achieved at the back rake angle around 45°。While the fragmentation volume of granite and sandstone show an upward trend with the subsequent increase of back rake angle in the whole analysis range. Fig. 4(c) shows the relationships between the specific energy and the back rake angle of different rocks. The curves drop sharply with the increase of back rake angle before 20°. After 20°, it stabilizes. Low specific energy demonstrates high rock fragmentation efficiency. Due to the relatively small angle between the cutter axis and the rock surface, and the unique shape of the cylinder side, the rock fragmentation is mainly plastic. With the gradual increase of the back rake angle, the lateral force of the cylindrical side of the cutter on the rock increases, and the brittle fracture of the rock increases. Combining the failure mode results at different back rake angles, it shows that the brittle failure is always accompanied by high crushing speed and crushing efficiency. This conclusion can be verified by the fragmentation analysis of different kinds of rocks.

No matter from the perspective of penetration depth, fragmentation volume, or specific energy, marble shows the best fragmentation effect, followed by sandstone, granite, and shale. Calculating the brittleness index of 4 types of rocks used in our study, Fig. 4(d) shows the results. It can be seen that the order of their brittleness from weak to strong is: shale, granite, sandstone, and marble. This order is consistent with the fragmentation effect and efficiency of these types of rocks under the impact load, indicating that the percussive drilling is more suitable for brittle stones. Brittleness is an essential property of rock. The brittleness index from compressive strength and tensile strength can be calculated as follows (Altindag, 2010; Yarali and Kahraman, 2011):

$$B = \frac{\sigma_c - \sigma_t}{\sigma_c + \sigma_t} \tag{2}$$

where B is the brittleness index, σ_c is uniaxial compressive strength, and σ_t is tensile strength.

3.2. Influence of drop height

Fig. 5 presents the curves of penetration depth, fragmentation volume, and specific energy versus drop height. Because the drop part first makes free-falling motion and then impacts the rock, the change in drop height reflects the variation in the final impact velocity. The higher the drop height, the greater the final impact velocity. The relationship between penetration depth and drop height is shown in Fig. 5(a). The penetration depth increases with the increase in the drop height, and the increasing rate is low when the drop height is small. Only when the impact velocity reaches a specific value can the rock be seriously penetrated. Indeed, there is also penetration depth when the impact velocity is low. This penetration is caused by the stress concentration generated by the tip of the PDC cutter. Fig. 5(b) and (c) show that the fragmentation volume rises with the increase of drop height while the specific energy decreases. All these curves demonstrate the significance of improving the impact velocity on enhancing the fragmentation effect. The changing trends of these curves have also resulted in the

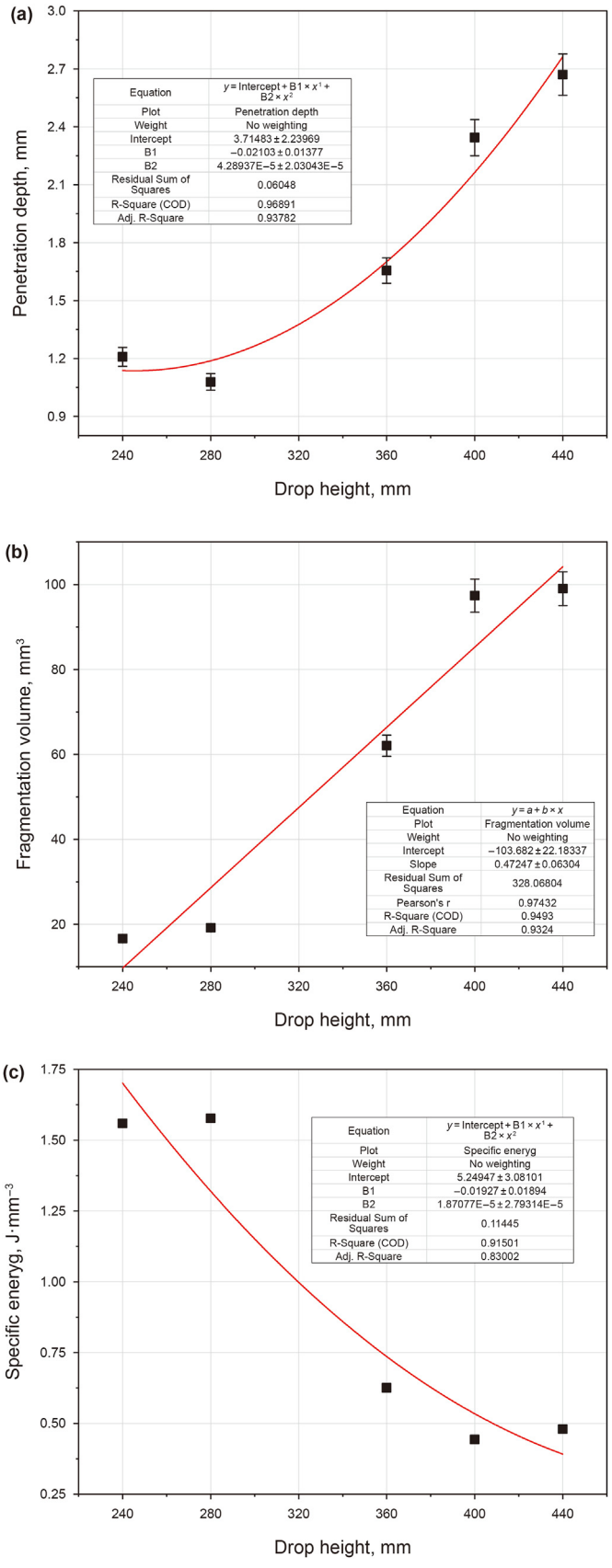

Fig. 5. The relationships between (**a**) penetration depth, (**b**)fragmentation volume, (**c**) specific energy and drop height.

change of failure mode. The surface topographies of craters at different drop height are shown in Fig. 6. The plastic failure can be seen clearly when the drop height is 240 and 280 mm. When the drop height increased to 320 mm, the plastic zone almost disappeared. Finally, the plastic area has been completely invisible when the drop height is higher than 360 mm.

3.3. Influence of drop mass

Fig. 7 shows the relationships between penetration depth, fragmentation volume, specific energy, and drop mass. Both penetration depth and fragmentation volume increase with the increase of drop mass while the specific energy decreases. These curves show that raising the mass of the impact body is beneficial to improving the fragmentation effect. However, the enhancement of the fragmentation effect in the evaluated range of drop mass is relatively small compared with that caused by impact velocity.

3.4. Influence of drop times

The impact times are also evaluated in our studies. And Fig. 8 demonstrates the relationships between penetration depth, fragmentation volume, specific energy, and the impact times. Both penetration depth and fragmentation volume increase linearly with the increase in impact times, which shows that increasing the times of impacts is useful for increasing the crushing volume and penetration depth. The linear curves of penetration depth and fragmentation volume versus impact times are formed for the following reason. Our tests use granite as samples to study the influence of impact times. The brittle granite is dominated by brittle failure under impact load. So, the cuttings fall away from the crater after each impact, thus the next impact encounters a brand new rock surface. However, the impact volume and depth will certainly not increase linearly as the impact times increase infield cases. Due to the holding effect of drilling fluid, the cuttings generated in the last impact inevitably affect the next impact effect. If the formation encountered is relatively poorly brittle, continuous impacts will increase the hardness of the compaction core, resulting in a reduction in crushing volume and depth. The drilling efficiency is gradually reduced with the increase of impact times, which can be seen from the curves of specific energy versus impact times. High fragmentation volume and penetration depth mean good drilling effect. With the increase of impact times, the increased crushing effect and the decreased drilling efficiency are contradictory. Therefore, it is necessary to find critical issues to formulate the drilling scheme and realize the balance between drilling effect and efficiency in practical application.

3.5. Fracture micrographs

To further understanding the fragmentation mechanism of rocks by impact load of a single PDC cutter, the fracture micrographs are observed by using Quanta 200F Scanning Electron Microscope (SEM). The observed slice is collected from the impacted granite with a drop height of 320 mm. Such a cylinder-shaped slice has a dimension of ∅ 25 mm × 6 mm, and the granite crater is on the top surface. Fig. 9 displays the SEM results around four points (defined in Fig. 6) in the cavity. P1 is located on the rock surface around the crater. We grab the micrograph near this point to compare with the microstructure of other crater areas. Micrograph at P1 indicated that the cut rock surface is generally flat and integrated. However, there are still concave-convex surfaces and folds in the micro-scale. It is mainly caused in the cut process by the heterogeneity of composition and the uneven distribution of mineral particles. P2 is set in the part of the plastic failure. It is easily seen that the surface is smooth, and the rock broke along the cleavage plane to form a river-shaped fracture. The crystal here is large in size and strength, and the impact load of the PDC cutter cannot produce transgranular cracks.

P3 is at the bottom of the crater. The rock fragmentation here is mainly intermittent intergranular failure. Stepped fractures also be formed. There is some debris scattered on the fracture surface. P4 is at the shallow part near the boundary of the crater. There are more typical stepped fractures. The step is parallel to the crack propagation direction and perpendicular to the crack surface, which creates the smallest additional free surface and requires the least energy. The formation mechanism of the step-like fracture surface is due to the existence of secondary cleavage. Therefore, the crack is not along a crystal face in the fracture process. It can also be seen that there are more debris on the fracture surface, which shows

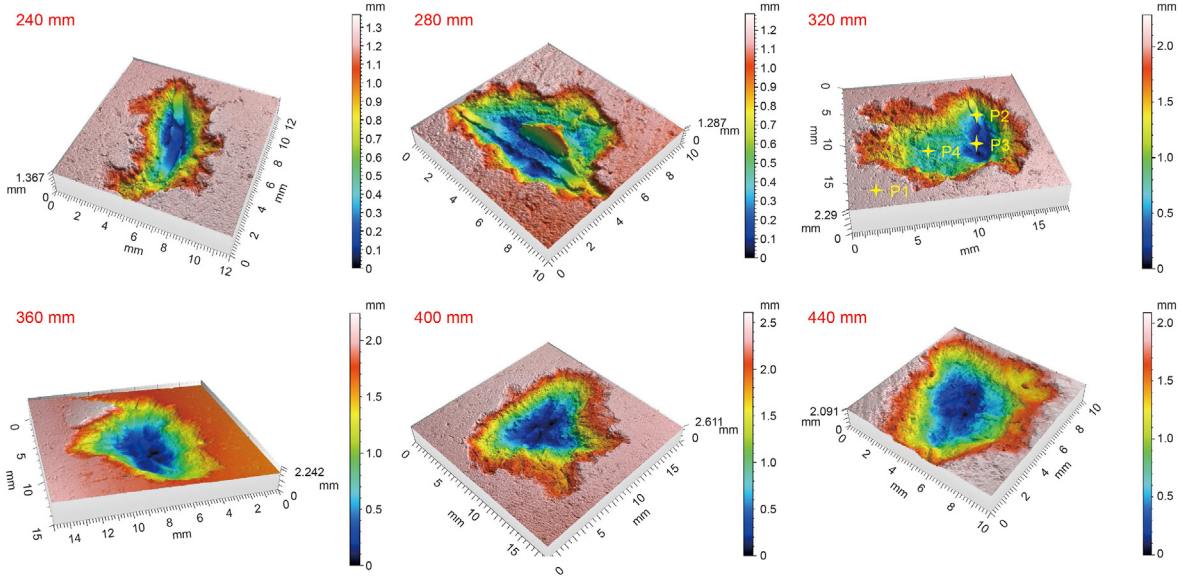

Fig. 6. Surface topography of granite crater at different drop height.

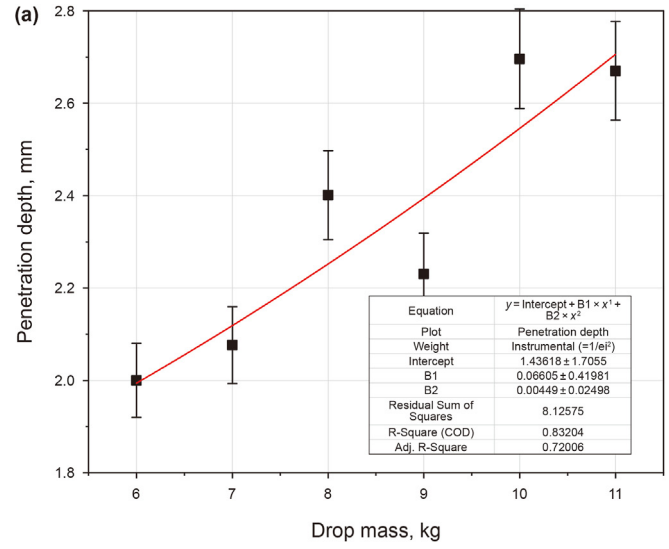

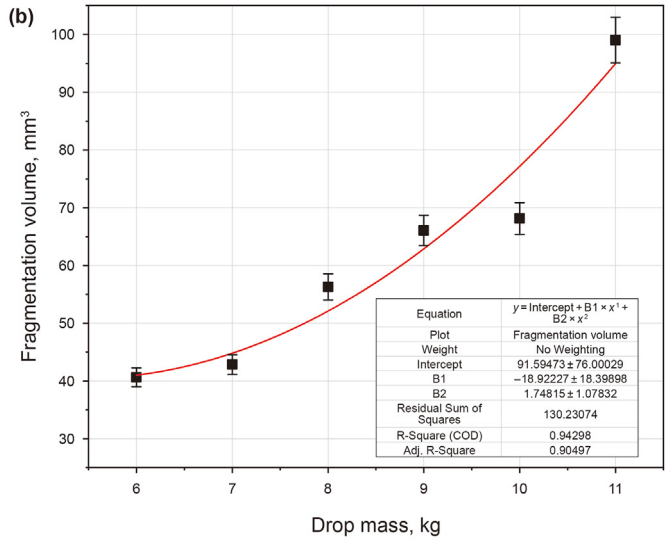

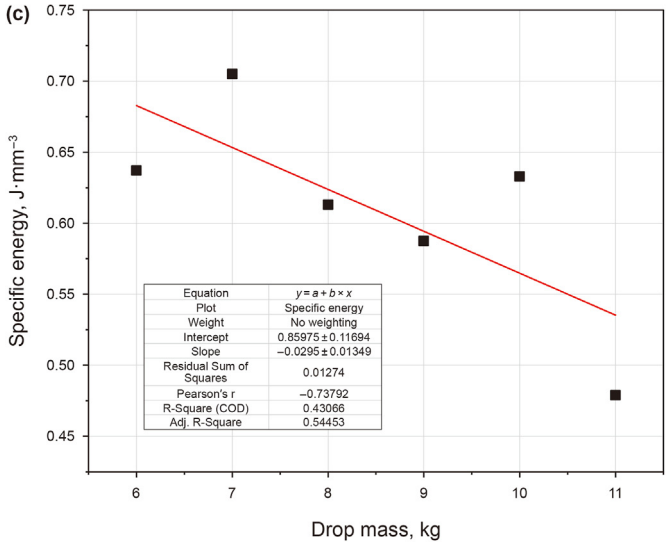

Fig. 7. The relationships between (**a**) penetration depth, (**b**)fragmentation volume, (**c**) specific energy and drop mass.

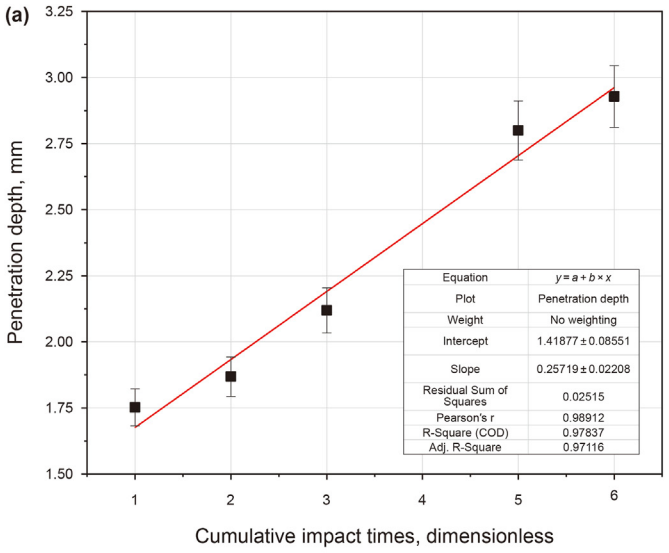

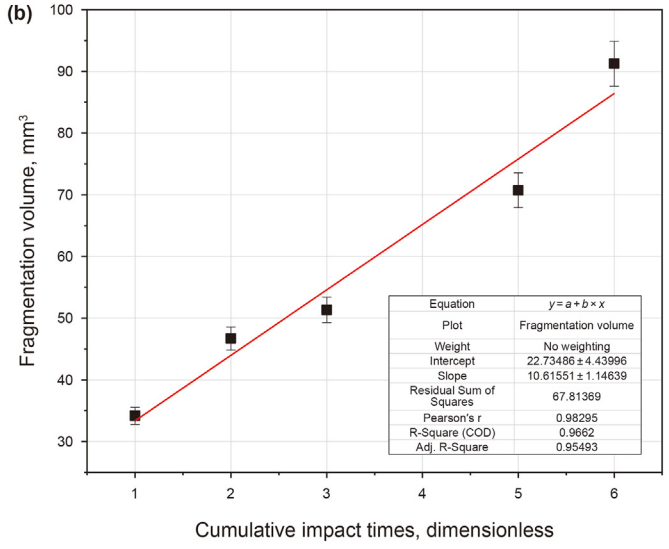

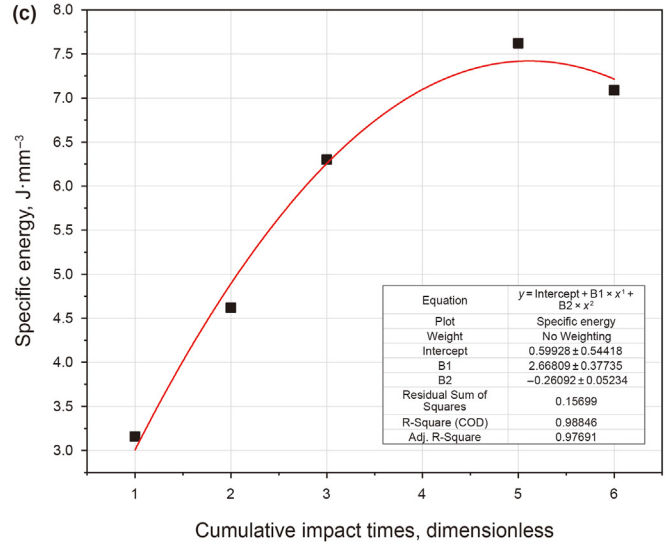

Fig. 8. The relationships between (**a**) penetration depth, (**b**)fragmentation volume, (**c**) specific energy and impact times.

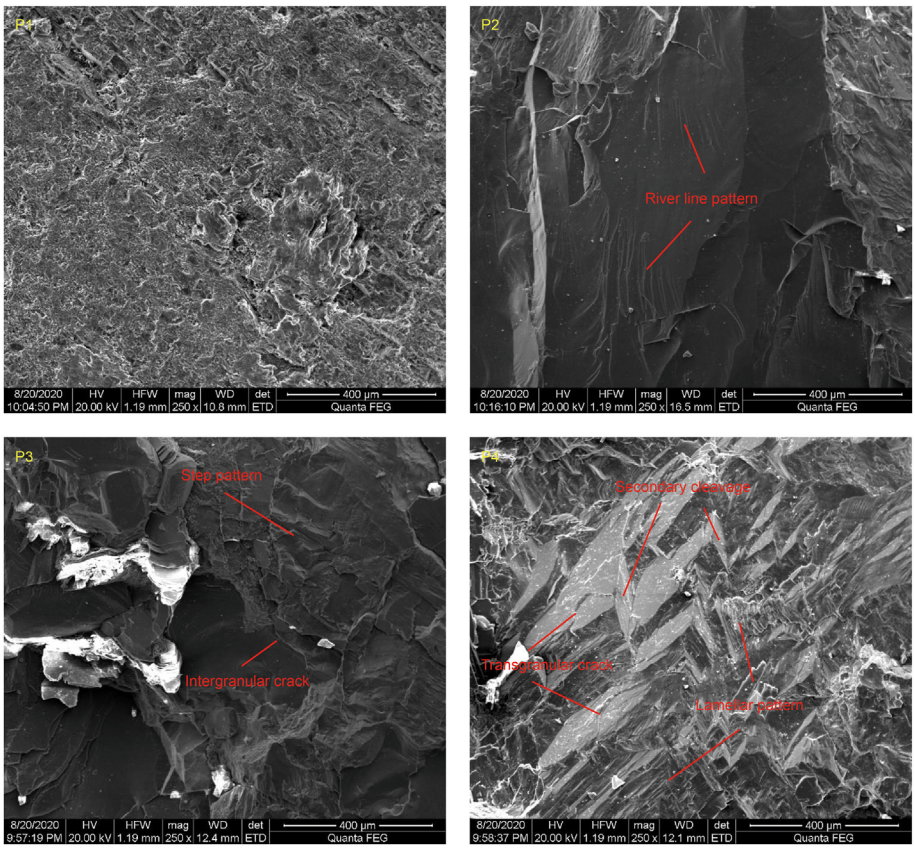

Fig. 9. Fracture micrographs at different position of the granite crater.

that the fracture is usually instantaneous under high strain rate loading. The rock is broken so instantaneously that it has enough deformation along the fracture surface, which generally produces irregular transgranular crack. There are also lamellar pattern fractures being found here. Compared with the micrograph at P4 and P3, it can be seen that more typical brittle fracture occurred in the shallow layer. The fracture morphology in shallow layer is more chaotic, the scale is more extensive, and the debris is much more. This phenomenon occurs because the shallow part is closer to the free surface, and the energy needed for rock fragmentation is more comfortable to release.

4. Subsurface cracks

Stress concentration under the impact load can produce many cracks under the rock fracture surface. These subsurface cracks can weaken the strength of the rock and create conditions for subsequent impact or shear action. Therefore, it is of great significance to conduct relevant research. Drop tests on the rock-like silica glass were performed to facilitate our observation of the distribution of subsurface cracks. And high-speed photography was used to capture the formation of craters and subsurface cracks.

Fig. 10 represents the pattern of subsurface cracks. The elevation view of the subsurface resembles a water wave expanding outwards. The crater is located at the place where the 'stone' is thrown. And the surface of the sample like the boundary of water where the 'wave' is blocked. The top view of the cracks is approximately fan-shaped and has a size of 1.5 cm $\times$ 2.5 cm. The crater is located at the root of the fan. The side view shows that the cracks are divided into two parts: one is the crack around the crater, the other is the crack beneath it. It is evident that the crack density around the crater is higher, and the longitudinal penetration depth of cracks reaches 3 cm. Combined with these three views, it can be found that the crack under the rock fracture surface is like a clamshell. The wave-like structure in the front view shows that the crack propagates discontinuously. The size of the rock cracks is much larger than the crater, which may mean that the crack system changes the stress state of rock better than the crushing pit to create conditions for subsequent drilling. The results further confirm the necessity of the research of subsurface cracks.

The propagation process of subsurface cracks is captured by high-speed photography, as shown in Fig. 11. Only the content in the observation window at different time is displayed to focus on the propagation process of subsurface cracks. When the PDC cutter touches the sample surface, the time is set to zero. As time went on, a crater was quickly formed under the PDC cutter. This process is going very fast. Then the clamshell-like subsurface cracks initiate and begin to expand at 200 μs. As the PDC cutter continues to press in, the clamshell-like crack develops continuously and nearly reaches the maximum size at 400 μs. Most of the kinetic energy of the falling part is converted into the surface energy required for crack propagation in this process. This is why the wave-like structure in the elevation view of Fig. 10 is produced. The energy accumulates as the lading of the PDC cutter, and then it is released by crack propagating. The above process cycles and the discontinuous cracks are formed. The growth rate of cracks gradually slows down from 200 to 400 μs. As the crack propagation almost stopped during 400–600 μs, the size of the cracks hardly changes. The kinetic energy of the falling part is mainly transformed into the compression energy of the sample in this stage. After 600 μs, the compression energy of the rock sample is released. The PDC cutter begins to rebound under the action of compression energy. This

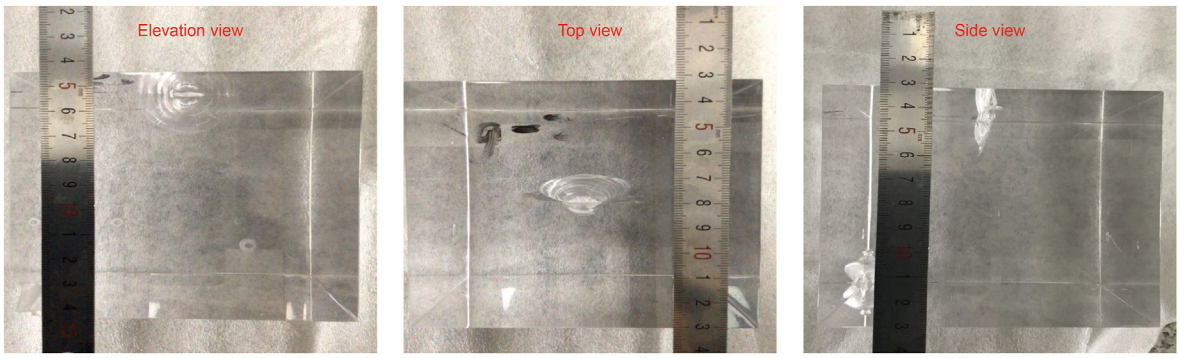

Fig. 10. Pattern of subsurface cracks.

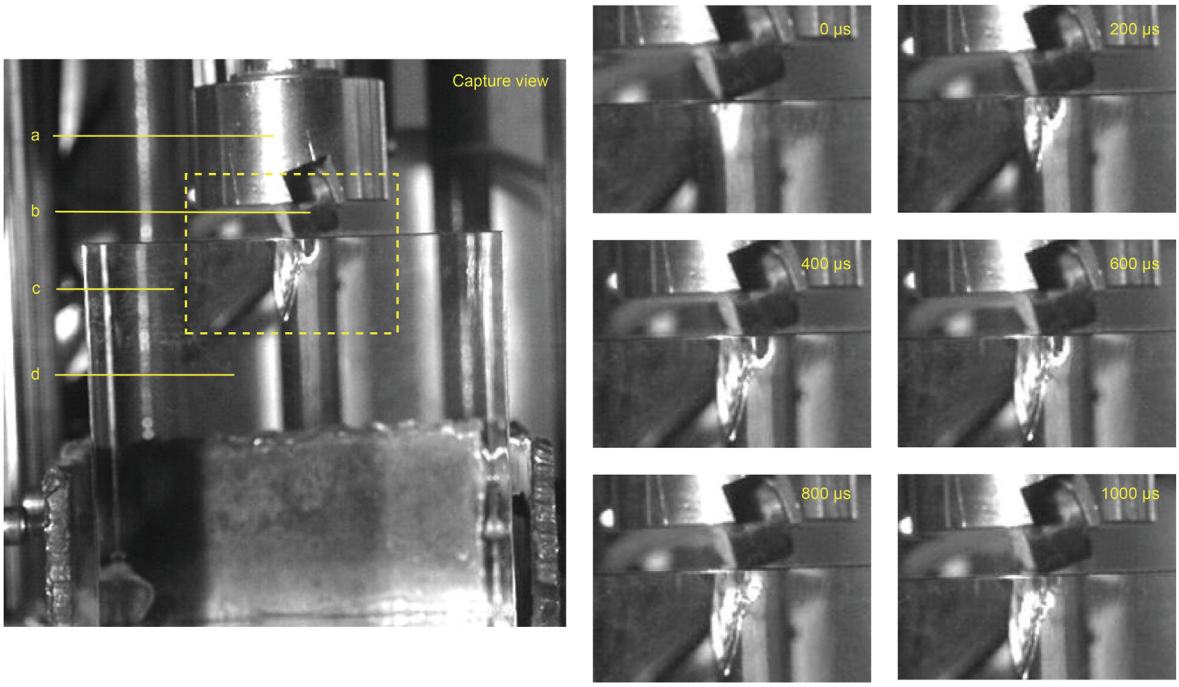

Fig. 11. Schematic diagram of subsurface crack propagation. a. clamping device, b. PDC cutter, c. observation window, and d. rock-like silica glass.

rebounding process ends at about 1000 μs. There was no change in the cracks during the early stages of the rebound . Only when the rebound stage was almost over, a few new cracks around the crater generated.

5. Conclusion

The rock failure mechanism under a single PDC cutter subjected to impact load is studied by conducting a series of drop tests in this work. Based on the discussions above, we can draw the following conclusions.

- There are two kinds of failure modes in craters: plastic failure and brittle failure. Compared to plastic failure, brittle failure is more efficient in breaking the rock. The occurrence of brittle failure is not only related to the rock type but also associated with the impact velocity, back rake angle, and direction of the PDC cutter.
- In percussive drilling of granite, PDC cutter with a 45° back rake angle has the best rock fragmentation effect, and rock breaking efficiency does not change much when it is higher than 20°. Increasing impact velocity and mass contribute to improving rock breaking effect and efficiency. Raising impact times can improve the rock breaking effect, but the rock-breaking efficiency continues to decrease.
- Typical brittle fracture micrographs are found in granite under the impact load, such as step pattern, river line pattern, and lamellar pattern. Compared with the bottom, the brittle fracture characteristics are more prominent in the shallow part of the crater. In the shallow part, the fracture morphology is more chaotic, the scale is more extensive, and the debris is much more. Transgranular cracks are also formed in the shallow part.
- Subsurface cracks are shaped like a clamshell, and the crater is located at the root of the clamshell. During the impact load, cavities formed first, and then subsurface cracks initiate and propagate. The propagation of subsurface crack is not continuous at a constant speed, but a discontinuous pulse propagation.

Declaration of competing interest

The authors declare that they have no known competing financial interests or personal relationships that could have appeared to influence the work reported in this paper.

Acknowledgment

The authors want to acknowledge the financial support of the China Postdoctoral Science Foundation (Grant No. 2021TQ0365) .

References

Abbas, R.K., 2018. A review on the wear of oil drill bits (conventional and the state of the art approaches for wear reduction and quantification). Eng. Fail. Anal. 90, 554–584. https://doi.org/10.1016/j.engfailanal.2018.03.026.

Ajibose, O.K., Wiercigroch, M., Akisanya, A.R., 2015. Experimental studies of the resultant contact forces in drillbit-rock interaction. Int. J. Mech. Sci. 91, 3–11. https://doi.org/10.1016/j.ijmecsci.2014.10.007.

Akbari, B., 2011. Polycrystalline Diamond Compact Bit-Rock Interaction. Memorial University of Newfoundland.

Akbari, B., Miska, S.Z., 2017. Relative significance of multiple parameters on the mechanical specific energy and frictional responses of polycrystalline diamond compact cutters. J. Energ. Resour.- ASME. 139 (2), 7. https://doi.org/10.1115/1.4034291.

Altindag, R., 2010. Assessment of some brittleness indexes in rock-drilling efficiency. Rock Mech. Rock Eng. 43 (3), 361–370. https://doi.org/10.1007/s00603-009-0057-x.

Beswick, A.J., Baron, G., Garnish, J.D., 1987. Drilling for hot dry rock reservoirs. Geothermics 16 (4), 429–432. https://doi.org/10.1016/0375-6505(87)90023-X.

Bilgin, N., Demircin, M.A., Copur, H., et al., 2006. Dominant rock properties affecting the performance of conical picks and the comparison of some experimental and theoretical results. Int. J. Rock Mech. Min. 43 (1), 139–156. https://doi.org/10.1016/j.ijrmms.2005.04.009.

Buyuksagis, I.S., Goktan, R.M., 2007. The effect of Schmidt hammer type on uniaxial compressive strength prediction of rock. Int. J. Rock Mech. Min. 44 (2), 299–307. https://doi.org/10.1016/j.ijrmms.2006.07.008.

Chen, J., Yue, Z., 2015. Ground characterization using breaking-action-based zoning analysis of rotary-percussive instrumented drilling. Int. J. Rock Mech. Min. 75, 33–43. https://doi.org/10.1016/j.ijrmms.2014.11.008.

Cheng, Z., Sheng, M., Li, G., et al., 2018. Imaging the formation process of cuttings: characteristics of cuttings and mechanical specific energy in single PDC cutter tests. J. Petrol. Sci. Eng. 171, 854–862. https://doi.org/10.1016/j.petrol.2018.07.083.

Cheng, Z., Sheng, M., Li, G., et al., 2019. Cracks imaging in linear cutting tests with a PDC cutter: characteristics and development sequence of cracks in the rock. J. Petrol. Sci. Eng. 179, 1151–1158. https://doi.org/10.1016/j.petrol.2019.04.053.

Depouhon, A., Denoel, V., Detournay, E., 2015. Numerical simulation of percussive drilling. Int. J. Numer. Anal. Model. 39 (8), 889–912. https://doi.org/10.1002/nag.2344.

Derdour, F.Z., Kezzar, M., Khochemane, L., 2018. Optimization of penetration rate in rotary percussive drilling using two techniques: taguchi analysis and response surface methodology (RMS). Powder Technol. 339, 846–853. https://doi.org/10.1016/j.powtec.2018.08.030.

Dong, G., Chen, P., 2018. 3D numerical simulation and experiment validation of dynamic damage characteristics of anisotropic shale for percussive-rotary drilling with a full-scale PDC bit. Energies 11 (6). https://doi.org/10.3390/en11061326.

Fan, Y.T., Huang, Z.Q., Gao, D.L., Li, Q., 2011. Experimental study of an Al2O3/WC-Co nanocomposite based on a failure analysis of hammer bit. Eng. Fail. Anal. 18 (5), 1351–1358, 10.106/j.engfailanal.2011.03.028.

Franca, L.F.P., 2011. A bit–rock interaction model for rotary–percussive drilling. Int. J. Rock Mech. Min. 48 (5), 827–835. https://doi.org/10.1016/j.ijrmms.2011.05.007.

Gee, R., Ramirez, T., Barton, S., et al., 2012. Reliable Hammer Motor Smashes its Way to Speedy Success in Brazil, IADC/SPE Drilling Conference and Exhibition. Society of Petroleum Engineers. https://doi.org/10.2118/151500-MS.

Hareland, G., Yan, W., Nygaard, R., et al., 2009. Cutting efficiency of a single PDC cutter on hard rock. J. Can. Petrol. Technol. 48 (6), 60–65. https://doi.org/10.2118/09-06-60.

Huang, K.L., Ai, Z.J., Yang, Y.X., et al., 2019. The improved rock breaking efficiency of an annular-groove PDC bit. J. Petrol. Sci. Eng. 172, 425–435. https://doi.org/10.1016/j.petrol.2018.09.079.

Hustrulid, W.A., Fairhurst, C., 1971. A theoretical and experimental study of the percussive drilling of rock Part II—force-penetration and specific energy determinations. Int. J. Rock Mech. Min. 8 (4), 335–356. https://doi.org/10.1016/0148-9062(71)90046-5.

Ji, Z., Shi, H., Li, G., et al., 2020. Improved drifting oscillator model for dynamical bit-rock interaction in percussive drilling under high-temperature condition. J. Petrol. Sci. Eng. 186, 106772. https://doi.org/10.1016/j.petrol.2019.106772.

Ji, Z., Shi, H., Dai, X., et al., 2021. Fragmentation characteristics of rocks under indentation by a single polycrystalline diamond compact cutter. J. Energ. Resour.- ASME. 143 (10), 100906. https://doi.org/10.1115/1.4050340.

Jiang, H.X., Du, C.L., Liu, S.Y., et al., 2014. Numerical simulation of rock fragmentation under the impact load of water jet. Shock Vib. https://doi.org/10.1155/2014/219489, 2014, 219489.

Jiang, L.S., Wu, Q., Wu, Q., et al., 2019. Fracture failure analysis of hard and thick key layer and its dynamic response characteristics. Eng. Fail. Anal. 98, 118–130. https://doi.org/10.1016/j.engfailanal.2019.01.008.

Jiang, H., Cai, Z., Zhao, H., 2020. Numerical study of hard rock breakage under indenter impact by the hybrid FDEM. Eng. Fract. Mech. 233, 107068. https://doi.org/10.1016/j.engfracmech.2020.107068.

Karfakis, M.G., Ouyang, H.J., 1994. Numerical modeling of rock-bit interaction in laminated formations. J. Energ. Resour.- ASME. 116 (1), 38–48. https://doi.org/10.1115/1.2906008.

Kuang, Y.C., Zhang, M.M., Feng, M., et al., 2016. Simulation and experimental research of PDC bit cutting rock. J. Fail. Anal. Prev. 16 (6), 1101–1107. https://doi.org/10.1007/s11668-016-0188-9.

Li, P., Zhang, H., Jiang, S.Y., et al., 2017. Analysis and testing of load characteristics for rotary-percussive drilling of lunar rock simulant with a lunar regolith coring bit. Shock Vib. (Pt.3), 3012749. https://doi.org/10.1155/2017/3012749.

Liao, M., Wiercigroch, M., Sayah, M., et al., 2021. Experimental verification of the percussive drilling model. Mech. Syst. Signal Process. 146, 107067. https://doi.org/10.1016/j.ymssp.2020.107067.

Liu, H.Y., Kou, S.Q., Lindqvist, P.A., 2008. Numerical studies on bit-rock fragmentation mechanisms. Int. J. GeoMech. 8 (1), 45–67. https://doi.org/10.1061/(ASCE)1532-3641(2008)8:1(45).

Pavlovskaia, E., Hendry, D.C., Wiercigroch, M., 2015. Modelling of high frequency vibro-impact drilling. Int. J. Mech. Sci. 91, 110–119. https://doi.org/10.1016/j.ijmecsci.2013.08.009.

Saksala, T., Gomon, D., Hokka, M., et al., 2014. Numerical and experimental study of percussive drilling with a triple-button bit on Kuru granite. Int. J. Impact Eng. 72, 56–66. https://doi.org/10.1016/j.ijimpeng.2014.05.006.

Song, H., Shi, H., Ji, Z., et al., 2019. The percussive process and energy transfer efficiency of percussive drilling with consideration of rock damage. Int. J. Rock Mech. Min. 119, 1–12. https://doi.org/10.1016/j.ijrmms.2019.04.012.

Song, H., Shi, H., Li, G., 2021. Numerical simulation of the energy transfer efficiency and rock damage in axial-torsional coupled percussive drilling. J. Petrol. Sci. Eng. 196, 107675. https://doi.org/10.1016/j.petrol.2020.107675.

Wang, S., Lam, K., Au, S., et al., 2006. Analytical and numerical study on the pillar rockbursts mechanism. Rock Mech. Rock Eng. 39 (5), 445–467. https://doi.org/10.1007/s00603-005-0075-2.

Wu, X., Huang, Z., Zhang, S., et al., 2019. Damage analysis of high-temperature rocks subjected to LN 2 thermal shock. Rock Mech. Rock Eng. 52 (8), 2585–2603. https://doi.org/10.1007/s00603-018-1711-y.

Yang, S., Zhang, N., Feng, X., et al., 2018. Experimental investigation of sandstone under cyclic loading: damage assessment using ultrasonic wave velocities and changes in elastic modulus. Shock Vib., 7845143 https://doi.org/10.1155/2018/7845143.

Yarali, O., Kahraman, S., 2011. The drillability assessment of rocks using the different brittleness values. Tunn. Undergr. Space Technol. 26 (2), 406–414. https://doi.org/10.1016/j.tust.2010.11.013.

Zhang, Q.B., Zhao, J., 2014. A review of dynamic experimental techniques and mechanical behaviour of rock materials. Rock Mech. Rock Eng. 47 (4), 1411–1478. https://doi.org/10.1007/s00603-013-0463-y.